The Use of Zeolites Synthesized from Fly Ash in Adsorption Chiller

Tarikul Hasan
tarikulhasan2011@gmail.com
Instituto Superior Tecnico, Universidade de Lisboa, Portugal
June 2021

Abstract: Adsorption chiller can produce cold energy, using the waste heat from the industries and the energy from the sun, thus reducing the energy consumption. A major waste, fly ash, can be converted to zeolite and used in adsorption chiller as adsorbent. In this thesis research, three different types of zeolites were synthesised from fly ash via a hydrothermal reaction in an alkaline solution (NaOH). Later, the samples (Na-A zeolites) were modified with K_2CO_3. XRD analysis suggests, desired zeolites have been formed properly, but other crystalline phases also exist. The determined specific surface area for Na-A zeolite (12 h) and Na-A zeolite (24 h) are 45 m^2/g and 185 m^2/g respectively, while the specific surface area for synthesized 13X zeolite is almost negligible. Water-isotherm for each of these sample were produced with the data obtained from DVS Vacuum-Surface Measurement System. Equilibrium adsorption at lower pressure steps was almost reached in less than 25 minutes for 13X zeolite and less than 20 minutes for Na-A zeolites, which is almost similar/better than silica gel. At usual operating conditions for adsorption chiller, available water vapor for evaporation for the synthesized samples is also very low, 1.73% and 1.27% for first and second operating conditions respectively for synthesized 13X zeolite, whereas no water vapor is available for evaporation for Na-A zeolite (12 h) and Na-A zeolite (24 h) zeolites. This analysis implies that among the synthesized materials, only 13X zeolite has some potential to be used in adsorption refrigeration system but cannot replace silica gel.

Key Word: Adsorption Chiller, Fly Ash, Zeolite, XRD, Specific Surface Area, Water Adsorption.

1.0. Introduction

The demand for cold energy is on the rise. The common refrigeration systems use electricity[1]. In 2019, 8.5% of total generated electricity was used for indoor cooling. The energy demand has tripled since 1990 [2]. It has been projected that number of AC unit will increase to 5600 million in 2050 from 1600 million in 2016 [3]. So, electricity consumption will also increase for the purpose of cooling. This electricity mainly comes from fossil fuels. In the year 2018, coal, natural gas and oil constituted 39%, 26% and 3% of total electricity generation [4]. It ultimately affects the environment. Also, HCFC is used as alternative to CFC in adsorption chiller to avoid damage to ozonosphere. But it has some greenhouse effects and also causes damage to ozonosphere[1].

There are many ways to desalinate the saline water such as multi-effect desalination, multi-stage flash desalination, membrane-based reverse osmosis [5]. These systems are very energy consuming. From 2010 to 2016, world's total water desalination capacity has increased by 9% each year [6]. This process is also very costly and adsorption desalination is a cheaper alternative[5].

We have solar energy and geothermal energy in the environment and waste energy from industries with low to very low temperature ranges. Adsorption chiller can utilize this heat with low temperature range. Adsorption refrigeration has a wide variety of adsorbents, including different physical and chemical adsorbents [1]. Physical adsorbents are driven by low grade heat, such as zeolite-water pair works in the range of 70–250 ∘C, silica gel-water pair works in the range of 55–120 ∘C, activated carbon-methanol pair works up to 120 ∘C temperature and activated carbon-ammonia pair works usually up to 150 ∘C temperature (can be used up to 200 ∘C or more) [1,7]. The used refrigerants have no ODP (Ozonosphere depletion

potential) and GWP (Greenhouse warming potential). But it is not as efficient as absorption refrigeration. The volume is also larger [1].

The performance of the adsorption chiller largely depends on the amount of adsorbed refrigerant, required time of adsorption/desorption, the temperature of adsorption and desorption, heat of adsorption and desorption, heat and mass transfer etc. The purpose of this thesis research is to synthesize Na-A and 13X zeolites from fly ash and analyse the potential application of these adsorbents compared to the performance of silica gel with regard to adsorption chiller. The objective of the work is as follows:

1. Synthesis of zeolite from fly ash by a hydrothermal reaction process and modification with K_2CO_3.
2. Characterization of the source material, silica gel and the synthesised materials, such as specific area measurement and XRD analysis.
3. Determination of adsorption isotherm and adsorption kinetics of the samples in DVS Vacuum- Surface Measurement System.
4. Performance analysis of the synthesised materials in regard of adsorption chiller with comparison to silica gel.

2.0. Literature Review and State of Art

2.1. Adsorption: Adsorption can be defined as adhesion of molecules of adsorbate on the surface of the adsorbent. There are basically two types of adsorptions, namely Physical and Chemical Adsorption. Physical adsorption occurs due to the van der walls bond. In contrast, the chemical adsorption occurs due to covalent bond and ionic bond. Physical adsorption releases low heat [8]. This enables us to use low temperature heat source in adsorption chiller.

2.2. Zeolite: Some of the most common physical adsorbents are activated carbon, activated carbon fiber, silica gel, and zeolite [1]. Our topic of interest is zeolite.

Zeolite is a microporous material that contains aluminium, silicon, and oxygen in its main three-dimensional crystalline structure and also includes cations and water [1]. The chemical formula of zeolite is $M_{y/n}[(AlO_2)_y(SiO_2)_m]zH_2O$ [1].

Here, y and m are all integer and m/y is equal to or larger than 1. n is the chemical valence of positive ion of M and z is the number of water molecules inside a crystal cell unit [1]. We have worked with Na-A zeolite and Na-X (13X) zeolite.

Na-A zeolite (LTA) is one of the family members of the aluminosilicate molecular sieves with chemical formula of this zeolite is $|(Na^{+}12(H_2O)_{27}|_8[Al_{12}Si_{12}O_{48}]_8$. The Si/Al ratio is 1 [10].

Na-X zeolite (FAU) is also one of the family members of aluminosilicate molecular sieves. The chemical formula of FAU is $|(Ca, Mg, Na_2)_{29}(H_2O)_{240}|[Al_{58}Si_{134}O_{384}]$ [11] with the Si/Al ratio in Na-X zeolite ranging between 1 to 1.5 [11].

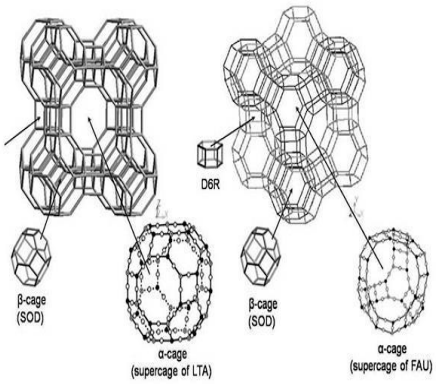

Figure-1: Framework of Na-A and Na-X Zeolite [9]

2.4. Adsorption Isotherm Models: There are different models for adsorption isotherm such as the Langmuir model, the Freundlich model, the Brunauer, Emmett, and Teller (BET) model etc. The BET model has been used to determine the specific surface area of the of the samples from nitrogen-isotherms (at -196 °C).

BET Model: It is applied to multi-layer adsorption. According to the BET theory, the equation for surface coverage is as follows [12],

$$a = \frac{a_m C \frac{P}{P_O}}{\left(1-\frac{P}{P_O}\right)\left[1+(C-1)\frac{P}{P_O}\right]} \quad \ldots\ldots\ldots\ldots\ldots\ldots 1$$

Here, "a" is the total amount of adsorbed vapour, "a_m" is the monolayer capacity, C is the BET constant, P is the pressure and P_0 is the saturation pressure [12]. C can be defined as following [13].

$$C = EXP(\frac{H_l - H_1}{RT}) \quad \text{.....2}$$

Here, $H_1$and H_l are, respectively, the adsorption enthalpies of the first layer and its subsequent ones. T is absolute temperature and R is the universal gas constant [13].

Plotting $(p/p_o)/(a(1–p/p_o))$ vs P/P_o in graph we can get the values for the constants of this equation such as C and a_m [12]. Surface area can be calculated from the following equation [12].

$S=a_m.L.\ \sigma_m/m$.....3

Here, S is specific surface area, L is avogadro constant, σ_m is molecular cross-sectional area and m is the mass of adsorbent [12].

2.5. Adsorption Isotherm Types: There are mainly 5 types of adsorption isotherm, namely Type I, Type II, Type III, Type IV and Type V. Among them Type I, Type II and Type III are for reversible adsorption types, whereas Type IV and Type V are for irreversible adsorption types. Another type is Type VI [14, 15]. These isotherms have significant use in this research work. The determined water isotherms are compared with these standard isotherm types to find out similar shapes and that can give us some important hints on the material's adsorption process, porosity type, etc.

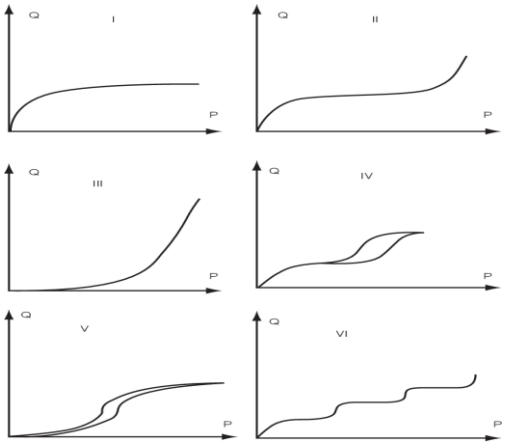

Figure-2: Adsorption isotherms in the classification [14].

2.6. Hysteresis: In physical adsorption hysteresis is observed mainly in mesoporous materials and results from capillary condensation. According to IUPAC, there are four types of hysteresis loops such as H1, H2, H3 and H4. Another additional type is H5 [15].

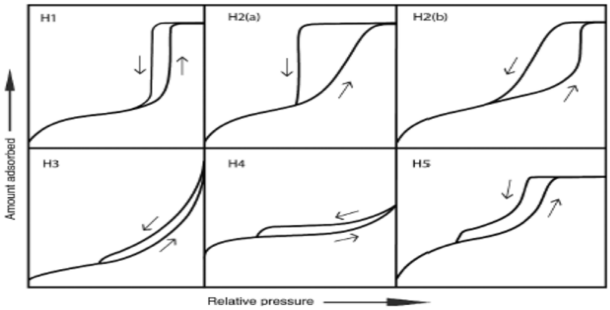

Figure-3: Classification of Hysteresis Loops [15]

2.7. Adsorption Refrigeration Process: The basic adsorption refrigeration cycle includes four steps.

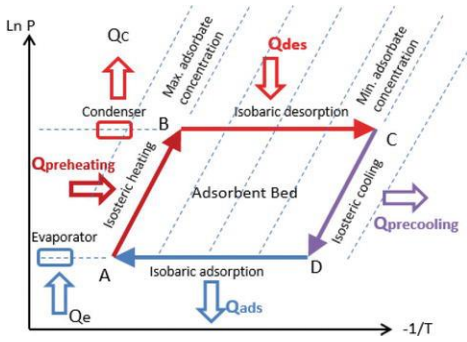

Figure-4: Ideal adsorption refrigeration cycle [16].

The pre-heating (A−B) section represents isosteric heating which result in increase of pressure and temperature. The desorption process (B−C) is an isobaric desorption process. In this section of operation, the temperature of the bed gradually increases, and refrigerant desorbs. The pre-cooling process (C−D) is isosteric cooling and it results in the decrease in temperature and pressure in the bed. The adsorption process (D−A) process comes after the isosteric cooling. In this period the effective cooling takes place due to the vaporization of the refrigerant in the evaporator[16].

2.8. Coefficient of Performance (COP): COP is defined by the ratio of the heat received by the evaporator (heat of vaporization) to the heat delivered for the heating process [17]. The equation is as follows:

$$COP = \frac{Q_e}{Q_{12}+Q_{23}} \text{……..(4)}$$

where Q_e is evaporator cooling heat (kJ), Q_{12} is isosteric heat of adsorption bed (kJ), Q_{23} is isobaric desorption heat of adsorption bed (kJ) [17].

2.9. Specific Cooling Power: Intensification of heat transfer of adsorption bed can greatly reduce the cycle time and that in turn can increase the specific colling power per kilogram of the adsorbent, SCP [1]. SCP can be defined by the following equation.

$$SCP = \frac{L\Delta x}{t_c} \text{……..(5)}$$

Here, L is the latent heat of vaporization, t_c is cycle time, and Δx is cycle adsorption quantity [1].

3.0. Experimental Method

3.1. Sample Preparation Method: Na-A zeolite (12 h) (Sample-1), Na-A zeolite (24 h) (Sample-2) and 13X zeolite (Sample-3) were prepared from fly ash. The Na-A zeolites were also modified with K_2CO_3. The fly ash was collected from a power plant in Poland. The composition includes SiO_2 = 45.50%, Al_2O_3 = 23.10%, Fe_2O_3 = 7.38%, CaO = 6.30%, MgO = 4.22%, Active CaO+MgO = 0.55%, S = 0.54%, SO_4^{2-} = 1.62%, TiO_2 = 0.72%, P_2O_5 = 0.29%, Mn_3O_4 = 0.17, Na_2O = 1.55%, K_2O = 2.96 and Combustion Loss = 6.42%.

3.1.1. Na-A Zeolite (12 h and 24 h) Preparation: 10 g fly ash was mixed with 12 g NaOH. The mixture was exposed to 550 °C temperature for 1 h. It was cooled downed to room temperature and grinded for 1 h. Then distilled water was added at 4: 1 ratio. This slurry was stirred in room temperature for 12 hours. It was exposed to 100 °C for 12 h and 24 h respectively. The samples were washed with distilled water and filtered. The obtained sample was dried in 100 °C for 12 h.

Modification with K_2CO_3 (Na-A Zeolite - 12 h): 5 g of zeolite was added with 2.5 g of K_2CO_3 and 25 ml of distilled water. It was stirred at room temperature for 24 h. Then it was dried at 60 °C. The last step was the calcination at 300 °C for 4 h.

Modification with K_2CO_3(Na-A Zeolite - 24 h): 100 g of zeolite was added with 50 g of K_2CO_3 and 500 ml of distilled water. It was stirred at room temperature for 10 h. Then it was dried at 105 °C. The last step was the calcination at 300 °C for 2 h.

3.1.2. 13X Zeolite Preparation: Fly ash was calcined at 800 °C to remove remaining carbon and volatile materials. The calcined sample was treated with HCl to dealuminate the fly ash and removed iron oxide to a certain extent. Then NaOH was added to fly ash at ratio of 1.5:1 (weight). This mixture was exposed to 550 °C for 1 h and later cooled down to room temperature. Later the sample was grinded and distilled water was added at the ratio of 10 g fly ash/100 mL water. The obtained mixture was stirred for hours. Then, it was allowed to settle at 90 °C for 6 h. After that, distilled water was used to wash the sample and filtered to get rid of the remaining sodium hydroxide, and later dried.

3.2. XRD Analysis: The XRD analysis was done at room temperature, using CuKα radiation. The used instrument was Panalytical Empyrean diffractometer equipped with PIXel3D detector. The applied 2θ range was 10-110 degree. The percentage of crystalline phases were determined by semi-quantitative method, and it was implemented in the HighScore software.

3.3. Surface Area Analysis: The surface area of the samples was determined using the BET model. The isotherms were developed with nitrogen adsorbent at -196 °C. The used instrument was Gemini V 2.00 (model 2380). All the samples were dehydrated overnight at 250 °C temperature.

3.4 Isotherm Determination: The DVS vacuum - surface measurement system was used for determination of the water adsorption isotherm. The method set in the software. We set parameters like system temperature, relative pressure step (P/Po), time duration for each step, the activation temperature (170 ^oC) for 90 minutes, incubator temperature and vapor flow rate. The data for dynamic sorption was created and recorded automatically in the software which was used for determining the isotherm.

4.0. Results and Discussion

4.1. XRD Analysis

4.1.1. Na - A Zeolite (Sample-1 and Sample-2)

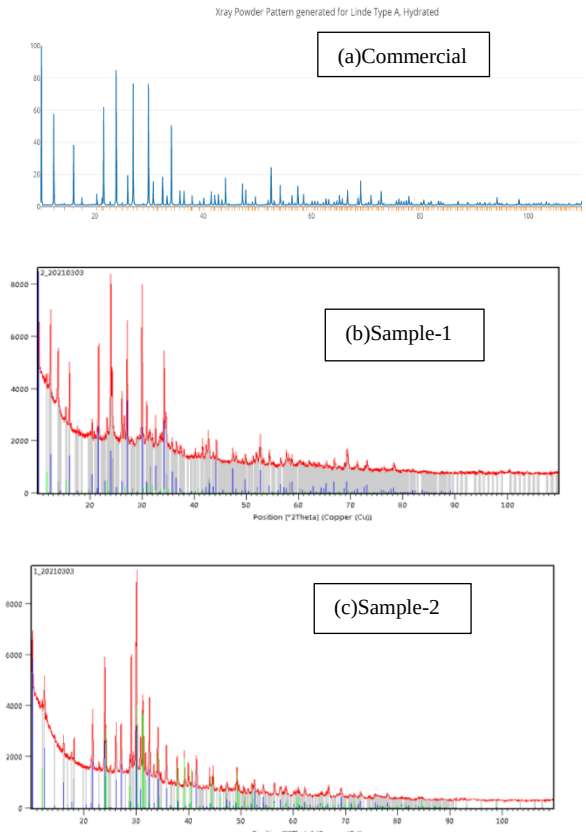

Figure-5: XRD Peaks Na-A Zeolite, (a) Commercial [18] (b) Sample-2 (c) Sample-2

Discussion: For commercial Na-A zeolite, we see peaks at 10.08, 12.4, 16.04, 21.64, 23.96, 26.08, 27.06, 29.92, 30.08, 32.58, 34.18, 35.78, 36.48, 41.46, 44.14, 47.24, 47.86, 52.58, 54.26, 57.46, 66.62 and 69.12. For Sample-1, we see reflections at 10, 12.5, 16.1, 21.6, 24,26,30, 32.8, 34.3, 35.8, 36.5, 41.5, 44.15, 47.25, 47.9, 52.6, 57.5, 66.7 and 69.12, which almost superimposes on the reflection peaks of commercial zeolite. For synthesized Na-A Zeolite (24 h), we see reflections at 10.08, 12.5, 16.04, 21.6, 24, 26,08, 27.1, 30, 32.6, 34.2, 35.8, 36.5, 41.5, 44.14, 47.25, 52.6, 54.3, 66.7 and 69.1, which almost superimposes on the reflection peaks of commercial zeolite. We see other peaks. Other detected phases are Potassium Aluminium Silicon Oxide and Sodium Calcium Aluminium Silicate Hydrate for sample-1, and Calcium Hydroxide and Potassium Hydrogen Carbonate for Sample-2.

4.1.2. 13X Zeolite

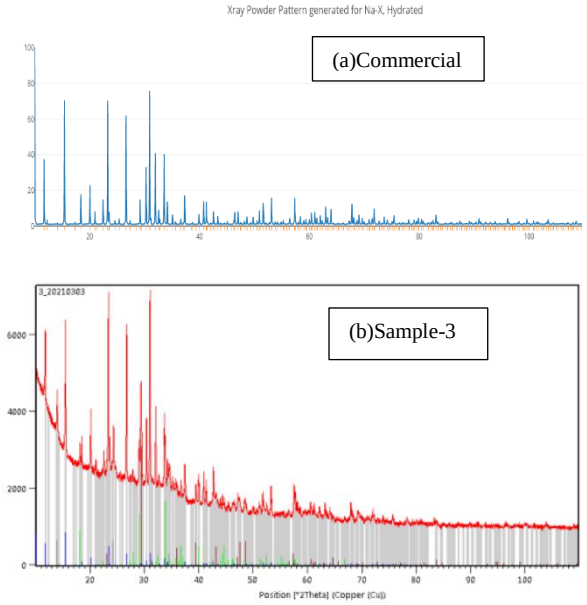

Figure-6: XRD Result Comparison 13X Zeolite, (a) Commercial[19] (b) Sample-3

Discussion: Figure-6 shows, for commercial zeolite, the peaks are at 9.9, 11.68, 15.42, 18.36, 20.04, 22.44, 23.34, 26.62, 29.2, 30.26, 30.88, 31.96, 32.58, 33.56, 34.08, 37.28, 40.76, 41.2, 51.6, 53.12, 57.38, 63, 64, 67.8 and 71.78. For our sample, we see reflections at 11.7, 15.45, 18.4, 20.04, 22.45, 23.4, 26.6, 29.2, 30.3, 30.8, 32,05, 32.6, 33.8, 34.1, 37.3, 40.7, 41.2, 51.6, 53.13, 57.4, 63.1, 68 and 72, which almost superimposes on the reflection peaks of commercial zeolite. We see other peaks as well. Other detected phases are Sodium Hydrogen Carbonate, $CaCO_3$, Sodium Aluminium Silicon Carbonate Oxide.

4.1.2. Surface Area Analysis

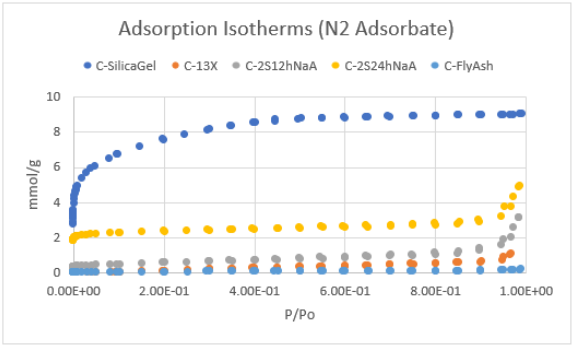

Figure-7: Adsorption Isotherm (at -196 °C)

Using the isotherms in figure 7, BET analysis has been done to determine the specific surface area of these samples. Determined specific surface area for Silica Gel is 613 m^2/g. For sample-1 and sample-2, the obtained specific surface area is 45 m^2/g and 185 m^2/g respectively, much lower than commercial Na-A Zeolite (850 m^2/g) [20]. It suggests, there are presence of non-porous crystalline and amorphous phases in synthesized samples. For both, synthesized 13X zeolite and Fly Ash, the obtained specific surface area is almost negligible. It suggests, the sample-3 mostly contains non-porous amorphous mass.

4.2. Adsorption Isotherm and Potential Use in Adsorption Chiller

4.2.1. Silica Gel

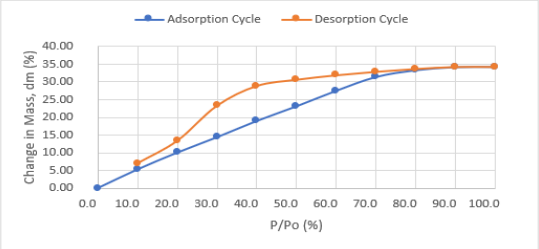

Figure-8: Adsorption Isotherm for Silica Gel (25 ºC)

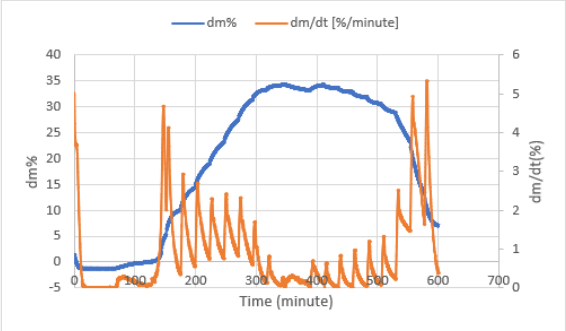

Figure-9: Adsorption Kinetics for Silica Gel (25 ºC)

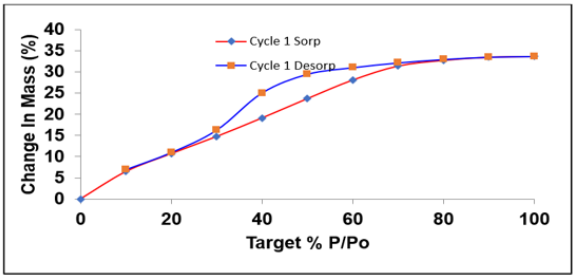

Figure-10: Adsorption Kinetics for Silica Gel (65 ºC)

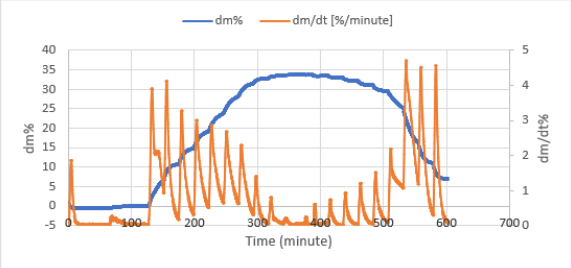

Figure-11: Adsorption Isotherm for Silica Gel (65 ºC)

Discussion:

Figure 8 to 11 show that the adsorption isotherm and kinetics for silica gel. This was achieved in 25 minutes time step. But adsorption kinetics suggests that it could have adsorbed and desorbed (for lower P/Po) more if time were increased. The isotherm resembles type IV isotherm. The hysteresis looks like a H2(b).

4.2.2. Synthesized Na – A Zeolite (12 h)

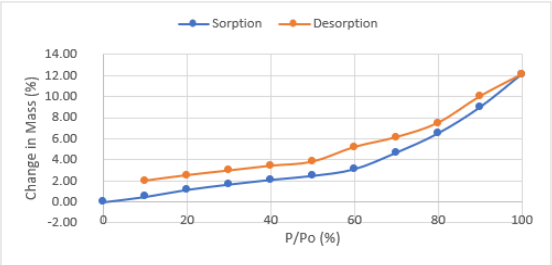

Figure-12: Adsorption Isotherm for Sample-1 (25 ºC)

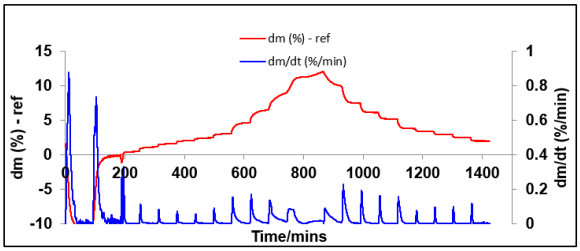

Figure-13: Adsorption Kinetics for Sample-1 (25 ºC)

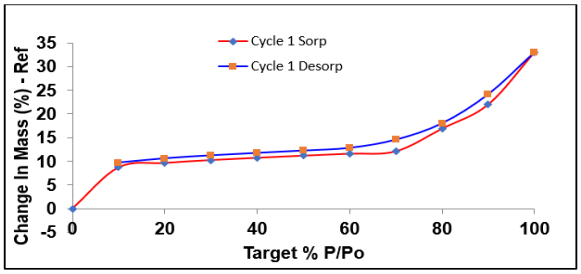

Figure-14: Adsorption Isotherm for Sample-1 (65 ºC)

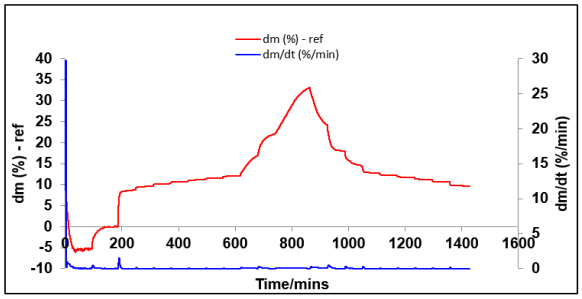

Figure-15: Adsorption Kinetics for Sample-1 (65 ºC)

Discussion:

Figure 12 to 15 show adsorption isotherm and kinetics for Sample-1. The isotherm resembles type IV. The adsorption in lower pressure region occurred due to presence of zeolite. The increase in adsorption in higher pressure region occurred due to capillary condensation in intergranular voids and hydration. The hysteresis does not close even at lower P/P_o for 25 ºC.

Potential Use in Adsorption Chiller: COP and SCP largely depend on how quickly the adsorbent can adsorb and desorb the refrigerant and at what amount, under the working condition [1, 17].

For this sample, the adsorption occurred for 60 minutes. But, if we look at adsorption kinetics for our sample in figure-13 and 15, it actually took less than 20 minutes to reach equilibrium (almost) at lower P/P_o, whereas for silica gel it was around 25 minutes. It implies that this sample will have better adsorption refrigeration cycle time compared to silica gel.

During adsorption, the pressure of the adsorbent bed is always lower, usually above 15% of the saturation pressure and sometimes can be as high as 45%. The temperature usually ranges between 25-40 ºC mostly [21, 22, 23, 24, 25]. Same papers suggest, during desorption of the refrigerant the temperature varies significantly (usually more than 65 ºC), whereas the pressure is usually less than 5% of the saturation pressure of the respective temperature and sometimes it can be around 10% or more as well. Based on these research works, two different working conditions have been considered.

First, for adsorption, if we consider 25 ºC temperature and 30% of saturation pressure (for water at 25 ºC), we observe that silica gel (14.37 %) adsorbed much more water vapor than this sample (1.66%) at this temperature and pressure. For desorption, if we consider the temperature is 65 ºC and pressure is 10% of the saturation pressure, the adsorption amount at this condition is 9.68% and 6.99% for sample-1 and silica gel respectively. So, at these conditions, the amount of water available for vaporization for sample-1 and silica gel should be 0% and 7.38% respectively. So, our sample cannot produce any cold energy.

Second, for adsorption, if we consider 25 ºC temperature and 20% of saturation pressure (for water at 25 ºC), and for desorption, if we consider the temperature is 65 ºC and pressure is 10% of the saturation pressure, the amount of water available for vaporization for sample-1 and silica gel should be 0% and 3.03% respectively. So, again, our sample cannot produce any cold energy.

4.2.3 Synthesized Na – A Zeolite (24 h)

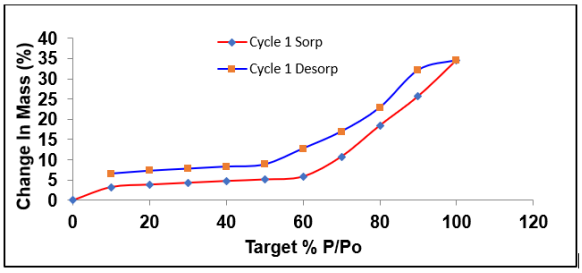

Figure-16: Adsorption Isotherm for Sample-2 (25 ºC)

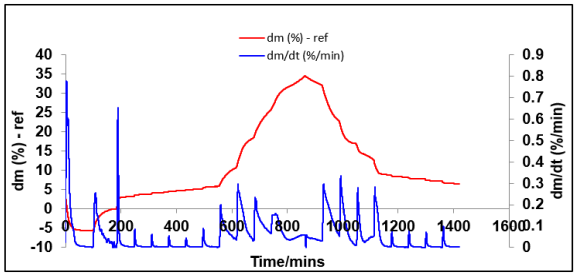

Figure-17: Adsorption Kinetics for Sample-2 (25 ºC)

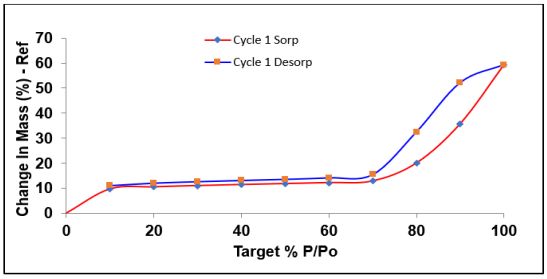

Figure-18: Adsorption Isotherm for Sample-2 (65 ºC)

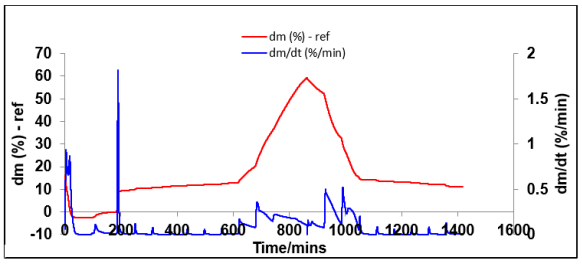

Figure-19: Adsorption Kinetics for Sample-2 (65 °C)

Discussion:

Figure 16 to 19 show the adsorption isotherm and kinetics for Sample-2. The isotherm resembles type IV. The adsorption in lower pressure region occurred due to presence of zeolite. The increase in adsorption in higher pressure region occurred due to capillary condensation in intergranular voids. It seems $KHCO_3$ also contributed, while hydration played a part probably. It has significant hysteresis issue. It does not close even at lower pressure for 25 °C.

Potential Use in Adsorption Chiller:

For this sample, the adsorption occurred for 60 minutes. But, if we look at adsorption kinetics for our sample in figure 17 and 19, it actually took less than 20 minutes to reach equilibrium (almost) at lower P/P_o, whereas for silica gel it was around 25 minutes. It implies that this sample will have better adsorption refrigeration cycle time compared to silica gel.

As I previously explained, based on the previous research works, I am considering two different working conditions for this sample as well.

First, for adsorption, if we consider 25 °C temperature and 30% of saturation pressure (for water at 25 °C), and for desorption, if we consider the temperature is 65 °C and pressure is 10% of the saturation pressure, then, the amount of water refrigerant available for vaporization at the evaporator in case of our sample and silica gel should be 0% and 7.38% respectively. So, our sample cannot produce any cold energy and replace silica gel as adsorbent for adsorption chiller.

Second, for adsorption, if we consider 25 °C temperature and 20% of saturation pressure (for water at 25 °C), and for desorption, if we consider the temperature 65 °C and pressure is 10% of the saturation pressure, then, the amount of water refrigerant available for vaporization at the evaporator in case of our sample and silica gel should be 0% and 3.03% respectively. So, again, our sample cannot produce any cold energy.

4.2.4 Synthesized 13X Zeolite

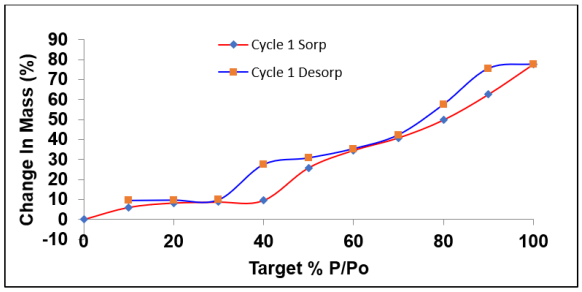

Figure-20: Adsorption Isotherm for Sample-3 (25 °C)

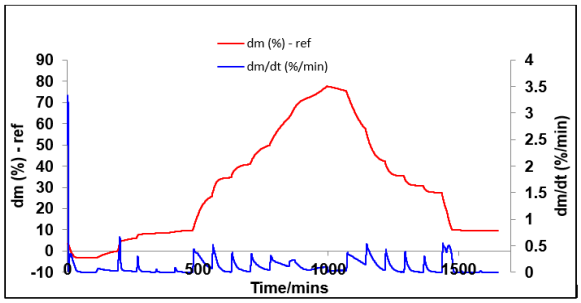

Figure-21: Adsorption Kinetics for Sample-3 (25 °C)

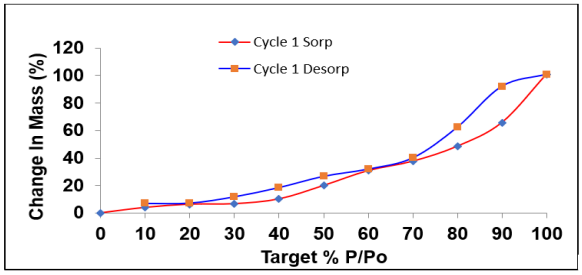

Figure-22: Adsorption Isotherm for Sample-3 (65 °C)

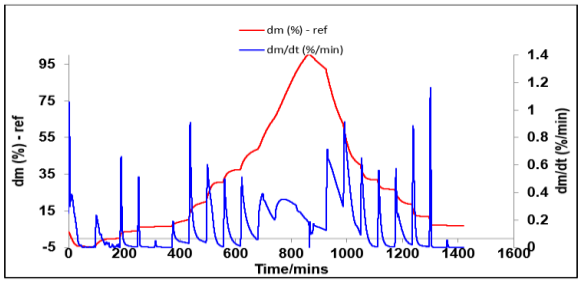

Figure-23: Adsorption Kinetics for Sample-3 (65 °C)

Discussion:

Figure 20 to 23 show that the adsorption isotherm and kinetics for Sample-3. The isotherm resembles type VI

isotherm. The adsorption in lower pressure region occurred due to presence of zeolite. The increase in adsorption in higher pressure region occurred due to capillary condensation in intergranular voids. It seems $NaHCO_3$ also contributed, while hydration played a part probably. It also has significant hysteresis issue.

Potential Use in Adsorption Chiller: For this sample, the adsorption occurred for 60 minutes. But, if we look at adsorption kinetics for our sample in figure 21 and 23, it actually took less than 25 minutes to reach equilibrium at lower P/P_o. For silica gel it was around 25 minutes. It implies, for this sample adsorption refrigeration cycle time will be similar or less, compared to silica gel.

As I previously explained, I am considering two different working conditions for this sample also.

First, for adsorption, if we consider 25 ^oC temperature and 30% of saturation pressure (for water at 25 ^oC), and, for desorption, if we consider the temperature is 65 ^oC and pressure is 10% of the saturation pressure, then the amount of water available for vaporization for sample-3 and silica gel should be 1.73% and 7.38% respectively. So, our sample can definitely produce some cold energy, but it cannot replace silica gel as adsorbent for adsorption chiller.

Second, for adsorption, if we consider 25 ^oC temperature and 20% of saturation pressure (for water at 25 ^oC), and for desorption, if we consider the temperature is 65 ^oC and pressure is 10% of the saturation pressure, then, the amount of water refrigerant available for vaporization at the evaporator in case of our sample and silica gel should be 1.27% and 3.03% respectively. So, again, our sample can produce some cold energy, but it cannot replace silica gel as adsorbent for adsorption chiller.

5.0. Conclusion

XRD analysis substantiated that the targeted compounds have been synthesized successfully. But the presence of other non-porous crystalline phases and amorphous phases is also evident. The impregnation of K_2CO_3 did not happen in desired manner totally and ended up developing other phases. The conversion percentage was low and for 13X zeolite, it was negligible. Considering the usual operating condition in adsorption chiller, it has been found that our synthesized Na-A zeolite samples cannot produce any cold energy, whereas the synthesized 13-X zeolite has some potential to create some cold energy. But it cannot replace silica gel in adsorption chiller.

Reference:

1. Wang, R., Wang, L., & Wu, J. (April 2014). Adsorption Refrigeration Technology: Theory and Application. John Wiley & Sons, Singapore Pte. Ltd. DOI:10.1002/9781118197448
2. Cooling, IEA. https://www.iea.org/reports/cooling. Last Visited: 23.01.2021
3. The Future of Cooling, IEA. https://www.iea.org/reports/the-future-of-cooling. Last Visited: 23.01.2021
4. Explore energy data by category, indicator, country or region, IEA. https://www.iea.org/data-and-statistics?country=WORLD&fuel=Electricity%20and%20heat&indicator=ElecGenByFuel Last Visited: 23.01.2021
5. WU, J,W. (2012). A study of silica gel adsorption desalination system. Thesis Report, School of Mechanical Engineering, Univetsity of Adelaide, Australia. https://digital.library.adelaide.edu.au/dspace/bitstream/2440/82463/8/02whole.pdf. Last Visited: 23.01.2021
6. Jia, X., Klemeš, J. J., Varbanov, P. S., & Alwi, S. R. W. (January 2019). Analyzing the Energy Consumption, GHG Emission, and Cost of Seawater Desalination in China. Energies. 12(463). DOI:10.3390/en12030463
7. Wolak, E., & Kraszewski, S. (October 2016). An overview of adsorptive processes in refrigeration systems. 1st International Conference on the Sustainable Energy and Environment Development (SEED), 10, Article 00104. https://doi.org/10.1051/e3sconf/20161000104.
8. Physical Adsorption vs. Chemisorption. http://www.separationprocesses.com/Adsorption/AD_Chp01b.htm Last Visited: 23.01.2021
9. Ríos, C. A., Williams, C. D., & Castellanos, O. M. (November 2012). Crystallization of low

silica Na-A and Na-X zeolites from transformation of kaolin and obsidian by alkaline fusion. Ingeniería y Competitividad, 14, No. 1, 9 – 22.

10. Julbe A., Drobek M. (2016) Zeolite A Type. In: Drioli E., Giorno L. (eds) Encyclopedia of Membranes. Springer, Berlin, Heidelberg. https://doi.org/10.1007/978-3-662-44324-8_604.
11. Julbe A., Drobek M. (2014) Zeolite X: Type. In: Drioli E., Giorno L. (eds) Encyclopedia of Membranes. Springer, Berlin, Heidelberg. https://doi.org/10.1007/978-3-642-40872-4_607-1.
12. Ambroz, F., Macdonald, T. J., Martis, V., & Parkin, I. P. (August 2018). Evaluation of the BET Theory for the Characterization of Meso and Microporous MOFs. Small Methods,2 (11). https://doi.org/10.1002/smtd.201800173.
13. Bashir, H., & Orouji, S. (2015). A new isotherm for multilayer gas adsorption on heterogeneous solid surfaces. Theoretical Chemistry Accounts,134, Article number 1594. https://doi.org/10.1007/s00214-014-1594-2.
14. Yahia, M. B., Torkia, Y. B., Knani, S., Hachicha, M. A., Khalfaoui, M., & Lamine, A. B. (April 2013). Models for Type VI Adsorption Isotherms from a Statistical Mechanical Formulation. Adsorption Science & Technology, 31(4), 341–357. https://doi.org/10.1260%2F0263-6174.31.4.341
15. Sotomayor, F. J., Cychosz, K. A., & Thommes, M, (2018). Characterization of Micro/Mesoporous Materials by Physisorption: Concepts and Case Studies. Accounts of Materials & Surface Research.
16. Elsheniti, M. B., Elsamni, O. A., Al-dadah, R. K., Mahmoud, S., Elsayed, E., & Saleh, K. (2018). Adsorption Refrigeration Technologies. IntechOpen, Sustainable Air Conditioning Systems, Edition: 1, Chapter: 4, 71-95. DOI: 10.5772/intechopen.73167.
17. Astinaa, I. M., Zidni, M. I., Hasugian, H. R., & Darmanto, P. S. (2018) "Experiment of adsorption refrigeration system with working pairs of difluoromethane and activated carbon modified by sulfuric and nitric acids", AIP Conference Proceedings, 1984 (1). https://doi.org/10.1063/1.5046599.
18. Xray Powder Pattern Generated for Na-X, Hydrated, Database of Zeolite Structures. https://europe.iza-structure.org/IZA-SC/pow_pat.php?STC=FAU&ID=FAU_2. Last Visited: 17/04/2021.
19. Xray Powder Pattern Generated for Na-A, Hydrated, Database of Zeolite Structures. https://europe.iza-structure.org/IZA-SC/pow_pat.php?STC=LTA&ID=LTA_0. Last Visited: 17/04/2021.
20. Rahmati, M., & Modarress, H. (July 2012). The effects of structural parameters of zeolite on the adsorption of hydrogen: a molecular simulation study. Molecular Simulation, 38(13). http://dx.doi.org/10.1080/08927022.2012.685941
21. Wang, X., He, Z., & Chua, H. T. (April 2015). Performance simulation of multi-bed silica gel-water adsorption chillers. Elsevier, International Journal of Refrigeration, 52, 32-41. https://doi.org/10.1016/j.ijrefrig.2014.12.016.
22. Sayfikar, M., & Behbahani-nia, A. (March 2013). Study of the performance of a solar adsorption cooling system. Energy Equipment and Systems, 1(1), 75-90. https://dx.doi.org/10.22059/ees.2013.2741.
23. Uyun, A. S., Akisawa, A., Miyazaki, T., Ueda, Y., & Kashiwagi, T. (October 2009). Numerical analysis of an advanced three-bed mass recovery adsorption refrigeration cycle. Elsevier, Applied Thermal Engineering, 29(14–15), 2876-2884. https://doi.org/10.1016/j.applthermaleng.2009.02.008
24. Sharafian, A., Mehr, S. M. N., Huttema, W., & Bahrami, M. (April 2016). Effects of different adsorber bed designs on in-situ water uptake rate measurements of AQSOA FAM-Z02 for vehicle air conditioning applications. Elsevier, Applied Thermal Engineering, 98, 568-574. https://doi.org/10.1016/j.applthermaleng.2015.12.060
25. Khanam, M., Jribi, S., Miyazaki, T., Saha B. B., & Koyama, S. (June 2018). Energy Analysis and Performance Evaluation of the Adsorption Refrigeration System. Energies, 11 (6), 1499. https://doi.org/10.3390/en11061499